Supplementary Information

Rapid, Accurate, and Reagent-Free Determination of Chlorine Concentration in Glass by Femtosecond LA-ICP-MS/MS with a Scanning Galvo Mirror System Using Hydrogen as Reaction Gas

Yoshitaka Saijo*, Makiko Murata, Junichi Hirata

Innovative Technology Laboratories, AGC Inc., 1-1 Suehiro-cho, Tsurumi-ku, Yokohama 230-0045, Japan.

* Corresponding author: E-mail: yoshitaka.saijo@agc.com
ORCID: 0000-0001-7292-5625

Table S1 Reported Cl mass fraction data (average values) for NIST SRM 610, 612, and 614. Data for NIST SRM 616 have not been previously reported.

	Analytical technique	Cl ($\mu g \cdot g^{-1}$)	n*)	1s**)	Reference	Date
SRM 610	CIC	273	5	21.8	1	2010
	CIC	100	-	30	2	2017
	LA-ICP-MS	262	-	4	3	2011
	LA-ICP-MS	229	-	14	3	2011
	EPMA	330	-	40	3	2011
	EPMA	470	2	-	4	1997
	EPMA	890	66	135	5	2017
	SIMS	438	-	-	6	2006
	TXRF	750	-	50	2	2017
	NI-NGMS	390	-	30	2	2017
SRM 612	CIC	88	5	12.3	1	2010
	CIC	20	-	10	2	2017
	LA-ICP-MS	179	-	4	3	2011
	LA-ICP-MS	221	-	35	7	2012
	EPMA	110	-	40	3	2011
	EPMA	200	-	200	8	1997
	EPMA	630	-	110	2	2017
	SIMS	131	-	-	6	2006
	TXRF	470	-	70	2	2017
	NI-NGMS	135	-	3	2	2017
SRM 614	IC	57	3	2.9	1	2010
	LA-ICP-MS	177	-	8	3	2011
	EPMA	81	-	40	3	2011
	SIMS	92	-	-	6	2006

*) n indicates the number of measurements; **) 1s represents the standard deviation. A hyphen indicates that no information was available.

Table S2 Operating conditions for CIC.

Combustion (AQF-2100H)	□
Furnace temperature	1100 ℃
Combustion gas	O_2
Combustion gas flow	400 mL·min^{-1}
Carrier gas	Ar
Carrier gas flow	200 mL·min^{-1}
Absorbent	NaOH
Absorbent volume	20 mL
Absorbent concentration	15 mM
Combustion time	11 min
Ion chromatography (ICS-2100)	□
Column	Dionex™ IonPac™ AG11-HC (4 mm i.d. × 50 mm) and Dionex™ IonPac™ AS11-HC (4 mm i.d. × 250 mm)
Eluent	KOH, Gradient mode, 26 mM from 0 to 10.0 min, 60 mM from 10.1 to 15.0 min, and 26 mM from 15.1 to 20.0 min
Column temperature	35 ℃
Eluent flow	1.0 mL·min^{-1}
Injection volume	200 μL
Suppression current	149 mA
Detection mode	Electric conductivity
Monitored ions	Cl^-
	PO_4^{3-} (as internal standard)

Table S3 Determined concentrations of chlorine in BAM-S005-A with different CIC conditions.

Combustion time (min) CuO	11 with	6 with	11 without
Determined Cl content ($\mu g \cdot g^{-1}$)	250	213	64
Certified Cl content ($\mu g \cdot g^{-1}$)		247 ± 33	

Table S4 Regression parameters (slope, intercept, R^2) for all runs (N = 1–6) under different LA-ICP-MS modes

Mode	Hydrogen addition–mass-shift			Hydrogen addition–on-mass			No-gas		
	Slope	Intercept	R^2	Slope	Intercept	R^2	Slope	Intercept	R^2
N = 1	5.86×10^{-5}	4.26×10^{-3}	0.9996	2.50×10^{-5}	3.46×10^{-4}	0.9736	9.28×10^{-5}	2.48×10^{-3}	0.9999
N = 2	5.99×10^{-5}	3.88×10^{-3}	1.0000	2.46×10^{-5}	3.42×10^{-4}	0.9744	9.37×10^{-5}	2.00×10^{-3}	0.9991
N = 3	6.38×10^{-5}	4.08×10^{-3}	1.0000	2.35×10^{-5}	5.40×10^{-4}	0.9780	9.34×10^{-5}	2.30×10^{-3}	0.9998
N = 4	6.41×10^{-5}	3.84×10^{-3}	0.9998	2.62×10^{-5}	2.00×10^{-4}	0.9835	9.41×10^{-5}	1.89×10^{-3}	0.9995
N = 5	7.74×10^{-5}	4.15×10^{-3}	0.9988	2.38×10^{-5}	7.59×10^{-4}	0.9832	9.43×10^{-5}	2.04×10^{-3}	0.9997
N = 6	7.43×10^{-5}	4.15×10^{-3}	0.9997	2.42×10^{-5}	6.64×10^{-4}	0.9731	9.42×10^{-5}	1.79×10^{-3}	0.9993

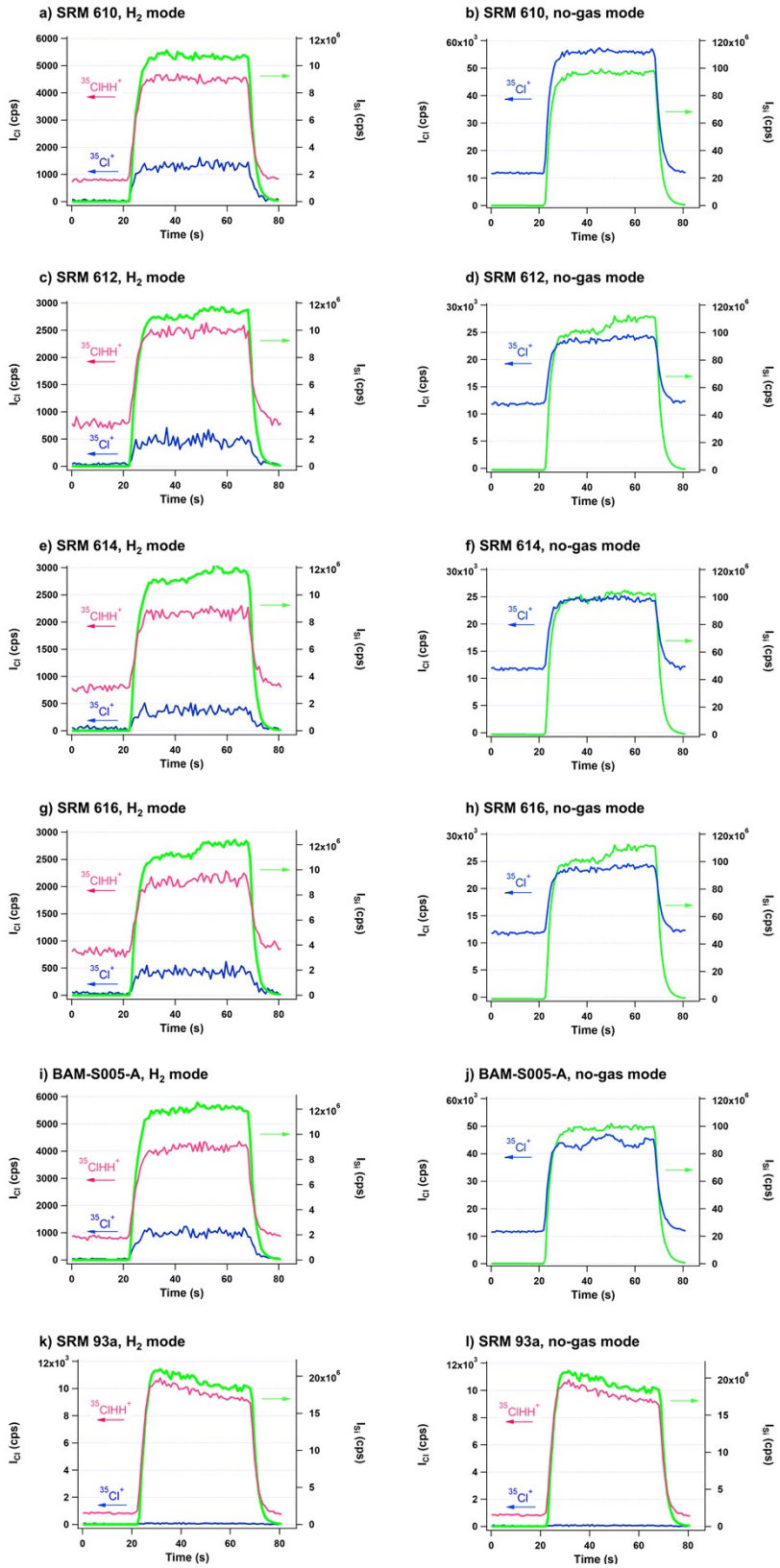

Fig. S1 Representative scan data (N = 1 per sample) illustrating signal-decay behavior; a)

SRM 610, H_2 mode; b) SRM 610, no-gas mode; c) SRM 612, H_2 mode; d) SRM 612, no-gas mode; e) SRM 614, H_2 mode; f) SRM614, no-gas mode; g) SRM616, H_2 mode; h) SRM 616, no-gas mode; i) BAM-S005-A, H_2 mode; j) BAM-S005-A, no-gas mode; k) SRM 93a, H_2 mode; and l) SRM 93a, no-gas mode. For each run, H_2 mass-shift and on-mass data were recorded simultaneously during the same ablation; no-gas mode was measured separately.

Table S5 LOD of chlorine ($\mu g \cdot g^{-1}$) for BAM-S005-A and SRM 93a under different LA-ICP-MS modes.

Sample	BAM-S005-A			SRM 93a		
Mode	Hydrogen addition–mass-shift	Hydrogen addition–on-mass	No-gas	Hydrogen addition–mass-shift	Hydrogen addition–on-mass	No-gas
N = 1	3.7	3.3	1.3	2.1	2.9	0.7
N = 2	3.7	3.3	1.2	2.2	3.1	0.7
N = 3	3.4	3.5	1.3	1.9	3.1	0.5
N = 4	3.4	3.5	1.2	2.0	3.3	0.5
N = 5	3.3	3.0	1.2	1.6	3.1	0.5
N = 6	4.0	2.9	1.1	2.1	3.3	0.5
Avg.	3.6	3.2	1.2	2.0	3.1	0.5
Standard deviation	0.3	0.2	0.1	0.2	0.2	0.1
Standard error	0.1	0.1	0.03	0.1	0.1	0.04
95% confidence interval	0.3	0.3	0.1	0.2	0.2	0.1

Table S6 LOQ of chlorine (μg·g^{-1}) for BAM-S005-A and SRM 93a under different LA-ICP-MS modes.

Sample	BAM-S005-A			SRM 93a		
Mode	Hydrogen addition–mass-shift	Hydrogen addition–on-mass	No-gas	Hydrogen addition–mass-shift	Hydrogen addition–on-mass	No-gas
N = 1	12.4	11.1	4.3	6.8	9.7	2.2
N = 2	12.3	10.9	4.1	7.3	10.4	2.2
N = 3	11.4	11.8	4.3	6.3	10.3	1.6
N = 4	11.3	11.6	4.1	6.7	11.0	1.5
N = 5	11.2	9.9	3.9	5.4	10.4	1.6
N = 6	13.5	9.8	3.8	7.0	11.0	1.5
Avg.	12.0	10.8	4.1	6.6	10.5	1.8
Standard deviation	0.9	0.8	0.2	0.7	0.5	0.3
Standard error	0.4	0.3	0.1	0.3	0.2	0.1
95% confidence interval	0.9	0.9	0.2	0.7	0.5	0.3

SI 1 Calculation of limit of detection (LOD) and quantification (LOQ)

The LOD and LOQ were calculated following Longerich et al.[9] using the standard deviation of the gas blank (σ_blank), the number of background and ablation points (Nb, Na), and the calibration sensitivity (S). S was calculated as the product of the calibration curve slope (Slope) and net ^{29}Si intensity of the sample ($I_{Si,\ sample,\ avg} - I_{Si,\ blank,\ avg}$), divided by the average SiO_2 mass% of the SRM 61x (71.6 mass%).

$$LOD = \frac{3\sigma\_blank}{S}\sqrt{\frac{1}{Nb} + \frac{1}{Na}} \quad (S1)$$

$$LOQ = \frac{10\sigma\_blank}{S}\sqrt{\frac{1}{Nb} + \frac{1}{Na}} \quad (S2)$$

$$S = Slope \times \frac{I_{Si,\ sample,avg} - I_{Si,\ blank,avg}}{Average\ SiO_2\ mass\%\ of\ the\ SRM\ 61x} \quad (S3)$$

A summary of the LOD/LOQ calculation parameters for each sample and measurement mode, using a single run (N = 1) as representative, is provided in Table S7. Parameters

include the number of background and ablation points (Nb, Na), standard deviation of the background (σ_blank, cps), calibration sensitivity (S, cps/(μg·g^{-1})), average background and ablation counts ($I_{Cl,\ blank.\ avg}$, $I_{Cl,\ sample,\ avg}$, cps), net signal (I_{Cl}, cps), and the calculated LOD and LOQ (μg·g^{-1}). These values demonstrate the reproducibility and transparency of the detection limit estimation.

Table S7 Summary of LOD/LOQ calculation parameters for each sample and mode

Sample	BAM-S005-A			SRM 93a		
Mode	Hydrogen addition–mass-shift	Hydrogen addition–on-mass	No-gas	Hydrogen addition–mass-shift	Hydrogen addition–on-mass	No-gas
Nb	25	25	25	25	25	25
Na	25	25	25	25	25	25
σ_blank (cps)	43	16	186	39	24	181
S (cps/(μg·g^{-1}))	9.8	4.2	121.2	16.3	7.0	232.3
$I_{Cl,\ blank.\ avg}$ (cps)	822	34	12032	836	40	12210
$I_{Cl,\ sample,\ avg}$ (cps)	4098	982	42424	10044	72	121748
I_{Cl} (cps)	3276	948	30392	9208	32	109539
LOD (μg·g^{-1})	3.7	3.3	1.3	2.1	2.9	0.7
LOQ (μg·g^{-1})	12.4	11.1	4.3	6.8	9.7	2.2

SI 2 Calculation of the conversion yield in hydrogen addition mode ($^{35}Cl^+ \rightarrow {}^{35}ClHH^+$)

The conversion yield in hydrogen addition mode ($^{35}Cl^+ \rightarrow {}^{35}ClHH^+$) was calculated using Eq. S4.

$$conversion\ yield\ (\%) = \frac{I_{Cl,\ mass-shift}}{I_{Cl,\ mass-shift} + I_{Cl,\ on-mass}} \times 100 \quad (S4)$$

Here, $I_{Cl,\ mass\text{-}shift}$ and $I_{Cl,\ on\text{-}mass}$ represent blank-subtracted net intensities acquired in the hydrogen addition–mass-shift mode and hydrogen addition–on-mass mode, respectively.

Table S8 Conversion yield in hydrogen addition mode ($^{35}Cl^+ \rightarrow {}^{35}ClHH^+$, n = 6, average ± 95% confidence interval)

Sample	SRM 610	SRM 612	SRM 614	SRM 616	BAM-S005-A	SRM 93a
Conversion yield (%)	74.9 ± 1.9	80.5 ± 0.6	80.8 ± 0.6	76.5 ± 0.8	76.8 ± 0.7	99.6 ± 0.1

SI 3-1 Statistical validation

To statistically validate the differences in chlorine concentrations among the different ICP-MS modes, we performed both analysis of variance (ANOVA) and Tukey's honestly significant difference (HSD) tests. ANOVA was used to determine if there were any statistically significant differences among the three test modes (hydrogen addition–mass-shift mode, hydrogen addition-on-mass mode, and no-gas mode). The results indicated a significant difference among the groups ($p < 0.05$). To further identify which specific groups differed from each other, we conducted Tukey's HSD post-hoc tests and compared all possible pairs of groups. The combination of ANOVA and Tukey's HSD provided a comprehensive analysis of the data, ensuring that our findings regarding the chlorine concentration measurements are robust and statistically sound.

SI 3-2 Results of statistical validation

The ANOVA results for BAM-S005-A showed that there was a statistically significant difference between groups ($F(2, 15) = 3.852$, $p = 0.0447$). The F-value (3.852) exceeded the F-critical value (3.682) at the 0.05 significance level, indicating that the null hypothesis of equal means was rejected. Tukey's HSD post-hoc tests revealed a significant difference between the hydrogen addition–on-mass mode and the no-gas mode.

For SRM 93a, the ANOVA results showed a statistically significant difference between groups ($F(2, 15) = 7803.81$, $p < 0.001$). The F-value (7803.81) far exceeded the F-critical value (3.682) at the 0.05 significance level, indicating that the null hypothesis of equal means was strongly rejected. The substantial difference in the mean chlorine concentrations, particularly the result falling below the LOD for the hydrogen addition–on-mass mode, highlights the disparities among the modes. Tukey's HSD post-hoc tests for SRM 93a showed significant pairwise differences among the groups.

References

1 Q. Wang, A. Makishima and E. Nakamura, *Geostand. Geoanal. Res.*, 2010, **34**, 175–183.

2 M. A. W. Marks, M. A. Kendrick, G. N. Eby, T. Zack, and T. Wenzel, *Geostand. Geoanal. Res.*, 2017, **41**, 107–122. DOI:10.1111/ggr.12128

3 K. P. Jochum, U. Weis, B. Stoll, D. Kuzmin, Q. Yang, I. Raczek, D. E. Jacob, A. Stracke, K. Birbaum, D. A. Frick, D. Günther and J. Enzweiler, *Geostand. Geoanal. Res.*, 2011, **35**, 397–429. DOI:10.1111/j.1751-908X.2011.00120.x.

4 N. J. G. Pearce, W. T. Perkins, J. A. Westgate, M. P. Gorton, S. E. Jackson, C. R. Neal and S. P. Chenery, *Geostand. Newsl.*, 1997, **21**, 115–144. DOI:10.1111/j.1751-908X.1997.tb00538.x.

5 M. A. W. Marks, M. A. Kendrick, G. N. Eby, T. Zack and T. Wenzel, *Geostand. Geoanal. Res.*, 2017, **41**, 107–122.

6 K. P. Jochum, B. Stoll, K. Herwig, M. Willbold, A. W. Hofmann, M. Amini, S. Aarburg, W. Abouchami, E. Hellebrand, B. Mocek, I. Raczek, A. Stracke, O. Alard, C. Bouman, S. Becker, M. Dücking, H. Brätz, R. Klemd, D. De Bruin, D. Canil, D. Cornell, C. J. De Hoog, C. Dalpé, L. Danyushevsky, A. Eisenhauer, Y. Gao, J. E. Snow, N. Groschopf, D. Günther, C. Latkoczy, M. Guillong, E. H. Hauri, H. E. Höfer, Y. Lahaye, K. Horz, D. E. Jacob, S. A. Kasemann, A. J. R. Kent, T. Ludwig, T. Zack, P. R. D. Mason, A. Meixner, M. Rosner, K. Misawa, B. P. Nash, J. Pfänder, W. R. Premo, W. D. Sun, M. Tiepolo, R. Vannucci, T. Vennemann, D. Wayne and J. D. Woodhead, *Geochem. Geophys. Geosyst.*, 2006, **7**. 1-44. DOI:10.1029/2005GC001060.

7 Q. C. Yang, K. P. Jochum, B. Stoll, U. Weis, D. Kuzmin, M. Wiedenbeck, H Traub, and M. O. Andreae. *Geostand. Geoanal. Res.*, 2012, **36**, 301–13. DOI: 10.1111/j.1751-908X.2012.00171.x.

8 N. J. G. Pearce, W. T. Perkins, J. A. Westgate, M. P. Gorton, S. E. Jackson, C. R. Neal, and S. P. Chenery. *Geostand. Newsl*., 1997, **21**, 115-144. DOI: 10.1111/j.1751-908X.1997.tb00538.x.

9 H.P. Longerich, S. E. Jackson, D. Günther. *J. Anal. At. Spectrom.,* 1996, **11**, 899-904. DOI: 10.1039/JA9961100899.